CERN - European Organization for Nuclear Research

LCD-Note-2011-009

The CLIC_SiD_CDR Detector Model for the CLIC CDR Monte Carlo Mass Production

C. Grefe[*†], A. Münnich[*]

[*] *CERN, Switzerland,* [†] *Rheinische Friedrich-Wilhelms-Universität Bonn, Germany*

June 2011

Abstract

The CLIC_SiD_CDR detector model for full simulation using GEANT4 is presented in this note. It is used for the Monte Carlo mass production for the CLIC CDR. The CLIC_SiD_CDR detector model is based on the SiD detector concept developed for the ILC.

This note is intended as a reference document for the geometry description, which is written in xml. All relevant numbers are presented in a comprehensive form and several illustrations are added to display the features of the detector model.

1. Introduction

This note describes the CLIC_SiD_CDR detector model, which is used for the simulation studies for the CLIC conceptual design report. The model is described as it is implemented in the GEANT4 [1, 2] based full simulation software SLIC [3] and differs from an actual engineering design. The differences are described in [4].

First a short overview of the CLIC_SiD_CDR detector model is given and then the different subdetectors are presented in more details in the following sections. The vertex and tracking detectors are described in section 3, the calorimeters and the muon system are described in section 4, the forward region is described in section 6 and the solenoid coil and the magnetic field are described in section 5. The final section gives more details on the full simulation software used. Materials which are differing from the default materials available in GEANT4 are described in Appendix A.

2. CLIC_SiD_CDR Overview

The CLIC_SiD_CDR detector model is a concept for a 4π multi-purpose detector for a future e^+-e^- linear collider. It is based on the SiD detector concept [5] developed for the ILC [6] and is designed for the particle flow paradigm [7]. With an overall length of 12.39 m and a total height of 12.50 m, the detector is rather compact. The parameters of the main detector components are listed in Table 1 and displayed in Figure 1.

The innermost part of the detector is the vertex detector with five layers in the barrel and four disks of silicon pixel detectors in the endcaps. It is surrounded by the main tracking system, consisting of five barrel layers of silicon strip detectors and four disks of silicon stereo-strip detectors on each side. The tracking system is completed by three additional silicon pixel disks in the forward region. A solenoidal field of 5 T is provided by a superconducting coil outside of the calorimeters.

Between the coil and the tracking systems are the calorimeters. The silicon-tungsten electromagnetic calorimeter (ECal) and the hadronic calorimeter (HCal) are highly granular sampling calorimeters, which are optimized for particle flow calorimetry. The HCal is instrumented with scintillator plates and steel is used as the absorber material in the endcaps. Tungsten is used as the absorber material in the HCal barrel in order to keep the size of the coil feasible.

The iron yoke, which surrounds the whole detector, is instrumented with resistive plate chambers (RPC). It helps with identifying muons and serves as a tail-catcher for the HCal.

The coverage for electromagnetic showers provided by the ECal is complemented by the luminosity calorimeter (LumiCal) and the beam calorimeter (BeamCal) in the far-forward region (see Figure 9). The design of the forward region is driven by the requirements for the final focusing quadrupole (QD0). The QD0 is placed behind the BeamCal and has to be supported by a large support tube from the tunnel walls in order to achieve the required stability [8].

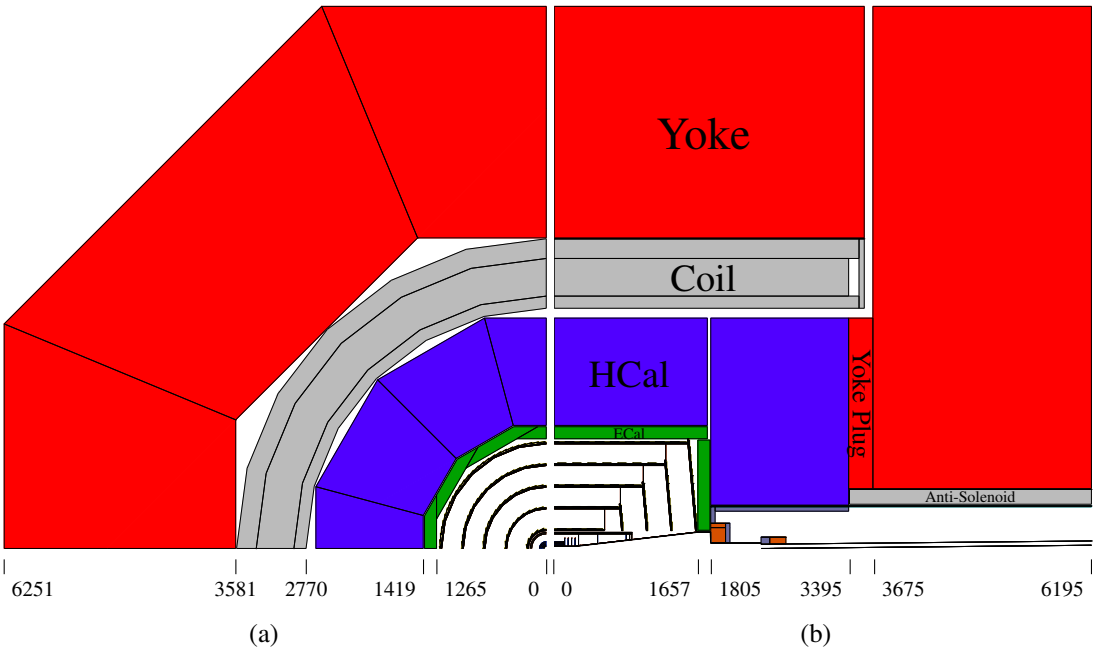

Figure 1: One quadrant of the CLIC_SiD_CDR detector model in the *xy*-plane (a) and in the *zx*-plane (b). Values are given in millimeter and resemble values shown in Table 1.

Table 1: Parameters for the main elements of the CLIC_SiD_CDR detector model. $z_{\text{min/max}}$ are the beginning and end in one half of the detector. The parameters $r_{\text{min/max}}$ are the radii of the inscribing circles for the polygons given in the last column. The polygon column gives the number of corners in case of polygonal shaped detector elements. All other elements are cylindrical.

	z_{min} [mm]	z_{max} [mm]	r_{min} [mm]	r_{max} [mm]	Polygon
ECal Barrel	0	1765	1265	1404	12
HCal Barrel	0	1765	1419	2657	12
Coil	0	3575	2770	3571	
Yoke Barrel	0	3575	3581	6251	8
ECal Endcap	1657	1796	210	1250	12
HCal Endcap	1805	3395	500	2657	12
Yoke Plug	3395	3675	690	2657	12
Yoke Endcap	3675	6195	690	6251	8
LumiCal	1805	1976	64	240	
BeamCal[A]	2486	2671	0	130	

[A] The BeamCal is centered around the detector axis. The holes for the incoming and outgoing beam pipes, which are not in the center, are described in section 6.3.

3. Tracking Detectors

The tracking system, consisting only of silicon detectors, is designed to provide excellent point resolution combined with low material budget. The pixel detectors (see section 3.1 and section 3.2) and the main tracking system (see section 3.4 and section 3.5) form an integrated system that provides at least ten precisely measured points for all tracks down to a polar angle of about 15° and at least six measured points down to a polar angle of about 8° (see Figure 2). The tracking performance is discussed in [9].

The layers of the tracking detectors are not segmented in the geometry model. Instead the segmentation is applied during the digitization step of the reconstruction in `org.lcsim` [10].

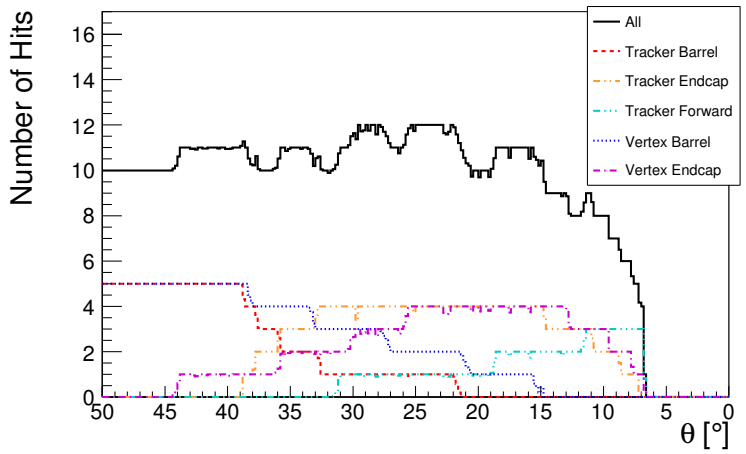

Figure 2: The coverage of the tracking systems with respect to the polar angle θ. Shown is the average number of hits created by a 500 GeV muon in full simulation. At least six hits are measured for all tracks with a polar angle down to about 8°.

3.1. Vertex Detector Barrel

The vertex barrel detector consists of five concentric layers. Each layer is made up by several modules as described in Table 2. Each module consists of 50 µm of silicon ($\approx 0.053\% X_0$) followed by 130 µm of carbon ($\approx 0.061\% X_0$) as support. The silicon is segmented into 20×20 µm^2 pixels. Figure 3 shows the arrangement of the layers and the modules in the vertex barrel detector.

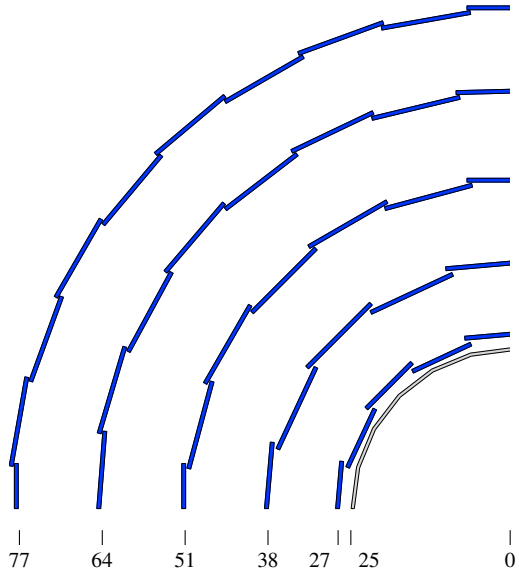

Figure 3: Layout of the vertex barrel detector in the xy-plane. Values are given in millimeter.

Table 2: Parameters for the vertex detector barrel layers. The number of modules N in the layer, the mean radius r of the layer, the half-length z of the module and width w of the module are given. Each module consists of a layer of 50 µm of silicon followed by 130 µm of carbon fiber.

Layer	N	r [mm]	z [mm]	w [mm]
1	18	27.0	98.5	9.8
2	18	38.0	98.5	13.8
3	24	51.0	98.5	13.8
4	30	64.0	98.5	13.8
5	36	77.0	98.5	13.8

3.2. Vertex Detector Endcap and Forward Tracking Disks

There are seven pixel disks covering the forward and far-forward region of the detector. The first four disks are close together and are considered part of the vertex detector. The three forward tracking disks extend the coverage of the tracker endcap to the beam pipe. All pixel disks consist of several trapezoidal modules as described in Table 3. Like in the vertex barrel each module consists of 50 µm of silicon ($\approx 0.053\% X_0$) followed by 130 µm of carbon ($\approx 0.061\% X_0$), with the silicon being segmented into 20×20 µm^2 pixels.

3.3. Vertex Detector Support

The vertex detector and the forward tracking disks are supported by a double-walled carbon fiber tube with an inner radius of 168.7 mm, an outer radius of 184.7 mm and a half length of 894.8 mm. Two carbon fiber disks close each end of the support tube. The first one is placed at 868.8 mm in z with an inner radius of 100.9 mm and the second one is placed at 894.3 mm in z with an inner radius of 103.9 mm. The outer radius for both disks is 168.7 mm. The thickness of each carbon fiber wall and disk is 0.5 mm.

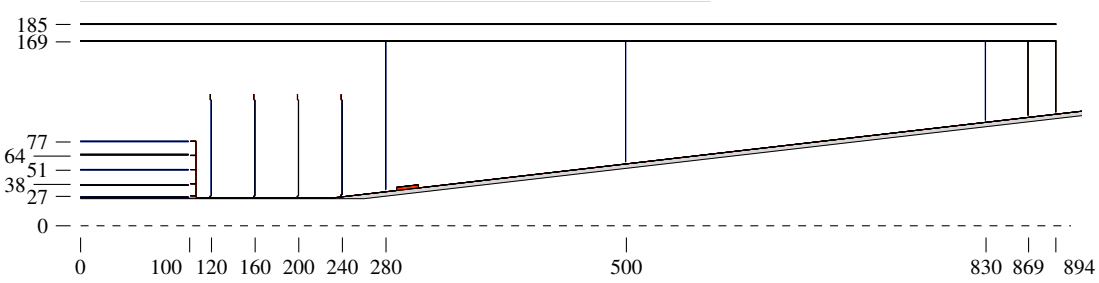

Figure 4: Layout of the vertex region. Shown are the vertex barrel layers, the vertex endcap disks and the forward tracking disks together with the vertex support, cabling and the central beam pipe. All values are given in millimeter.

Table 3: Parameters for the vertex endcap and forward tracking disks. The number of trapezoidal modules N, the inner radius r_{in}, the outer radius r_{out}, the inner width w_{in}, the outer width w_{out} and the position in z of the modules are given. Each module consists of a layer of 50 µm of silicon followed by 130 µm of carbon fiber.

Disk	N	r_{in} [mm]	r_{out} [mm]	w_{in} [mm]	w_{out} [mm]	z [mm]
1	16	27.0	115.0	10.8	45.1	120.0
2	16	27.0	115.0	10.8	45.1	160.0
3	16	27.0	115.0	10.8	45.1	200.0
4	16	28.1	115.0	11.3	45.1	240.0
5	16	32.8	168.7	13.1	66.2	280.0
6	16	58.2	168.7	23.3	66.2	500.0
7	16	96.4	168.7	38.6	66.2	830.0

3.4. Tracker Barrel

The main tracking detector consists of five layers of silicon strip detectors. The overall layout of the layers is described in Table 4. Each layer is made from several square modules with a size of $97.8 \times 97.8\,\text{mm}^2$. Each module consists of 0.3 mm of sensitive silicon ($\approx 0.32\%\, X_0$) and 2.6 mm of support and electronics ($\approx 0.19\%\, X_0$). A detailed description of the material in each module can be found in Table 5(a).

The silicon strips run along the z-direction and, with a length of 92.03 mm, span almost the whole module. Their pitch is 25 µm and every second strip is read out. The readout pitch is thus 50 µm.

3.5. Tracker Endcap

The tracker endcap consist of four silicon stereo strip layers. Each layer consists of several rings of trapezoidal modules. The rings are arranged to follow a conical shape (see Figure 5(b)). A detailed description of the layout of the disks can be found in Table 6.

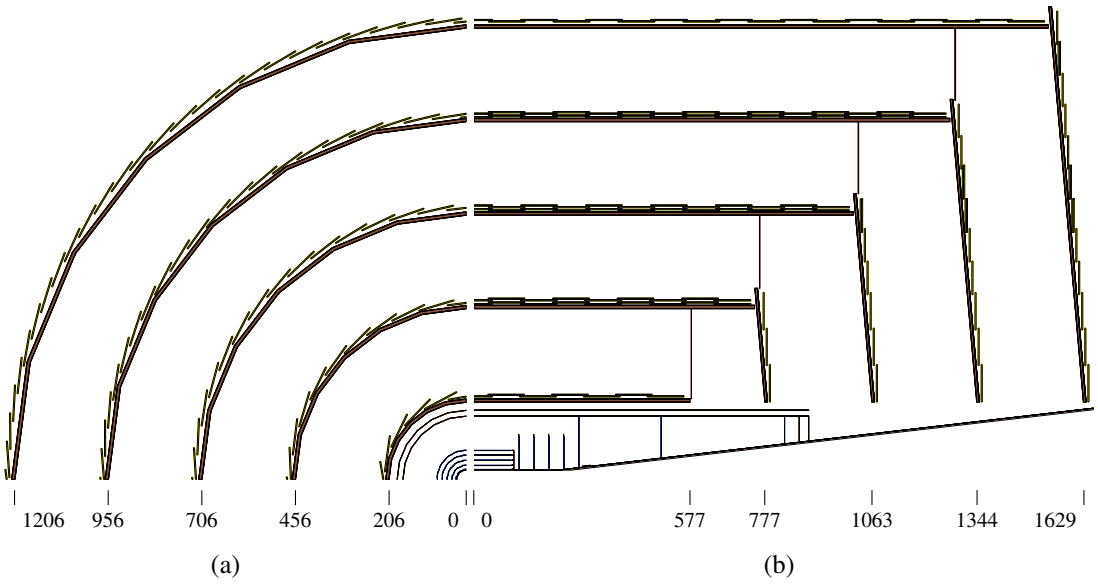

Figure 5: Layout of the tracking system in the xy-plane (a) and in the zx-plane (b). The main tracker modules are displayed in yellow and support structures are displayed in brown. A detailed view of the vertex detector can be found in Figure 3 and Figure 4. Values are given in millimeter.

Table 4: Parameters for the barrel tracker layers. The number of modules in the layer N in z and ϕ, the mean radius of the layer r and the half-length of the layer z are given. Each module consists of 300 µm of silicon and 2.6 mm of support material (see Table 5(a)).

Layer	N_z	N_ϕ	r [mm]	z [mm]
1	13	20	230.0	578.0
2	17	38	483.0	749.8
3	23	58	725.5	1013.9
4	29	80	988.5	1272.3
5	35	102	1239.0	1535.7

Each module has two layers of 0.3 mm of sensitive silicon, amounting to about 0.64% X_0, and other material simulating support and electronics described in detail in Table 5(b). The modules used in the inner three rings have a radial extent of 100.1 mm and the modules in the outer rings have a radial extent of 89.8 mm.

Like for the tracker barrel, the silicon strips have a width of 25 µm and the readout pitch is 50 µm. The strips in the first sensitive layer are perpendicular to one side of the trapezoid, while the strips in the second sensitive layer are perpendicular to the other side of the trapezoid. The layout of the inner and outer modules is chosen, such that in both cases the stereo angles between

Table 5: Materials and corresponding thicknesses d in each of the modules in the tracker barrel (a) and in the tracker endcap (b). Ordered as seen from the interaction point. The carbon fiber and ROHACELL31 used in the main tracker modules have only half of their nominal densities and thus twice the radiation length.

(a) Tracker barrel module

Material	d [µm]
Copper	3.8
Kapton	38.0
Silicon (passive)	4.8
Silicon (sensitive)	300.0
Carbon Fiber (50%)	160.0
Epoxy	175.0
ROHACELL31 (50%)	1800.0
Carbon Fiber (50%)	160.0
PEEK	200.0

(b) Tracker endcap module

Material	d [µm]
Copper	5.2^{A}/ 7.9^{B}
Kapton	51.0^{A}/ 78.0^{B}
Silicon (passive)	4.8
Silicon (sensitive)	300.0
Carbon Fiber (50%)	160.0
Epoxy	175.0
ROHACELL31 (50%)	1800.0
Carbon Fiber (50%)	160.0
Silicon (sensitive)	300.0
Silicon (passive)	4.8.0
Kapton	51.0^{A}/ 78.0^{B}
Copper	5.2^{A}/ 7.9^{B}

A Material in the inner three rings.
B Material in the outer rings.

the two sensitive layers is 12°.

3.6. Tracker Support

The tracker barrel layers are supported by cylinders of 8.075 mm ROHACELL31 coated on both sides with 0.5 mm of carbon fiber. The ROHACELL used in the tracker barrel support only has 15% of the nominal density of ROHACELL31 to represent a lower density foam. The corresponding total radiation length for each layer is thus 0.48% X_0. The positions of the support cylinders are described in Table 7(a).

Each of the endcap disks is supported by a cone of 3.5 mm of ROHACELL31, which is coated on both sides by 0.5 mm carbon fiber, amounting to about 0.50% X_0. The positions of the endcap supports are given in Table 7(b).

3.7. Cabling and Readout

A ring of G10 with a radial extent of 0.2 mm ($\approx 0.12\%\, X_0$) and a z-extent of 5 mm ($\approx 3.1\%\, X_0$) is placed on both ends of each vertex barrel layer to represent connectors. Connectors for the vertex endcap disks are simulated as a ring of G10 with a radial extent of 0.9 mm ($\approx 0.56\%\, X_0$) and a z-extent of 0.2 mm ($\approx 0.12\%\, X_0$) on the inside and another ring with a radial extent of 4.9 mm ($\approx 3.1\%\, X_0$) and a z-extent of 0.2 mm ($\approx 0.12\%\, X_0$) on the outside of each disk.

Table 6: Parameters for the tracker endcap disks, which are made of trapezoidal modules that are arranged in rings. The number of modules N, the inner radius r_{in}, the outer radius r_{out}, the two widths of the trapezoid $w_{\text{in/out}}$ and the position in z of the modules within the ring are given. The material budget of the modules is described in Table 5(b).

Disk	N	r_{in} [mm]	r_{out} [mm]	w_{in} [mm]	w_{out} [mm]	z [mm]
1	24	206.7	306.7	72.2	93.3	787.1
	32	304.0	404.0	72.2	93.3	778.8
	40	399.2	499.2	72.2	93.3	770.5
2	24	206.7	306.7	72.2	93.3	1073.3
	32	304.0	404.0	72.2	93.3	1065.0
	40	399.2	499.2	72.2	93.3	1056.7
	40	493.5	583.5	90.5	109.4	1048.5
	48	580.7	670.7	90.5	109.4	1041.1
	54	658.7	748.7	90.5	109.4	1033.7
3	24	206.7	306.7	72.2	93.3	1353.8
	32	304.0	404.0	72.2	93.3	1345.5
	40	399.2	499.2	72.2	93.3	1337.2
	40	493.5	583.5	90.5	109.4	1329.0
	48	580.7	670.7	90.5	109.4	1321.6
	54	658.7	748.7	90.5	109.4	1314.2
	58	748.4	848.4	90.5	109.4	1306.8
	64	829.2	919.2	90.5	109.4	1299.5
	68	913.4	1003.4	90.5	109.4	1292.2
4	24	206.7	306.7	72.2	93.3	1639.2
	32	304.0	404.0	72.2	93.3	1630.8
	40	399.2	499.2	72.2	93.3	1622.6
	40	493.5	583.5	90.5	109.4	1614.3
	48	580.7	670.7	90.5	109.4	1606.9
	54	658.7	748.7	90.5	109.4	1599.6
	58	748.4	841.4	90.5	109.4	1592.2
	64	829.2	919.2	90.5	109.4	1584.9
	68	913.4	1003.4	90.5	109.4	1577.6
	72	996.0	1096.0	90.5	109.4	1570.2
	78	1079.2	1169.2	90.5	109.4	1562.9
	84	1161.9	1251.9	90.5	109.4	1555.6

The cables are routed along the beam pipe (see section 6.3) and are simulated as copper coating around the beam pipe with a thickness of 50 µm between the end of the vertex barrel detector ($z = 100$ mm) and a z of 290 mm. At a z of 290 mm a cone of G10 with a radial extent of 3 mm and a z-extent of 20 mm is placed around the beam pipe to simulate services. Another copper cable around the beam pipe with a linearly decreasing thickness from 100 µm to 40 µm

Table 7: Positions of the tracker barrel support layers (a) and the conical supports for the tracker endcap disks (b).

(a) The inner radius of the layer r and the half-length of the layer z are given. The thickness is 9.075 mm.

Layer	r [mm]	z [mm]
1	206.0	577.3
2	456.0	749.8
3	706.0	1013.8
4	956.0	1272.3
5	1206.0	1535.7

(b) The inner surfaces of the cones are defined by the positions $z_{1/2}$ and the radii $r_{1/2}$. Their thickness perpendicular to the inner surface is 4.5 mm.

Disk	z_1 [mm]	z_2 [mm]	r_1 [mm]	r_2 [mm]
1	750.4	777.0	510.4	206.2
2	1014.4	1063.2	763.8	206.2
3	1272.9	1343.7	1015.7	206.2
4	1536.6	1629.1	1263.8	206.2

is placed between a z of 310 mm and the end of the conical beam pipe ($z = 1656$ mm).

Copper disks are placed at the end of the vertex barrel, representing cables connecting each layer with the readout cable around the beam pipe. The thickness of the copper disks decreases from inside to outside after each layer. The thickness decreases from 57 µm between the first two layers, to 31 µm between layers two and three, to 16 µm between layers three and four, to finally 7 µm between the last two layers.

The readout cables for the main tracker are simulated as disks composed of copper and G10. They are placed at each end of the tracker barrel layers and connect to the next layer. The positions and thicknesses are given in Table 8.

Table 8: Parameters for the main tracker readout. The inner radius of the disk r_{in}, the outer radius of the disk r_{out}, the position z, the thickness d of the G10 and the copper is given together with their combined radiation length X/X_0.

Layer	r_{in} [mm]	r_{out} [mm]	z [mm]	d_{G10} [µm]	d_{Cu} [µm]	X/X_0 [%]
1	215.0[A]	456.0	590.4	570	38	0.62
2	510.0	706.0	762.9	1020	68	1.10
3	763.0	956.0	1026.9	1080	72	1.17
4	1013.0	1206.0	1285.3	1860	124	2.01

[A] The production version has a value of 279 mm, which was corrected later.

3.8. Material Budget

The accumulated material budget of the tracking region is shown in Figure 6. The vertex detector, including the beryllium beam pipe (see section 6.3) and the carbon fiber support tube, amount to about $1\%\,X_0$ for an incident angle of 90°. The total material of all tracking systems

corresponds to about 7% X_0. Which rises to about 17% X_0 in the transition region between barrel and disk detectors at polar angles between 30° and 40°.

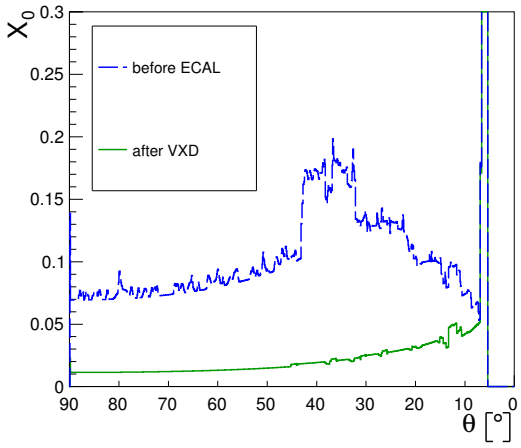

Figure 6: The radiation length X_0 in the tracking region, including the beam pipe, with respect to the polar angle θ. The conical beam pipe causes the sharp peak at $\theta \approx 7°$ (see section 6.3).

4. Calorimeters

Table 9: Parameters for the different calorimeter layers. The number of identical layers N_{Layers}, the total thickness of each layer d_{Layer}, the absorber material, its thickness d_{Abs}, the sensitive material and its thickness d_{Sens} are given.

	N_{Layers}	d_{Layer} [mm]	Absorber	d_{Abs} [mm]	Sensitive	d_{Sens} [mm]
ECal	1	1.00			Silicon	0.32
	20	3.75	Tungsten	2.5	Silicon	0.32
	10	6.25	Tungsten	5.0	Silicon	0.32
HCal Barrel	75	16.50	Tungsten	10.0	Scintillator	5.00
HCal Endcap	60	26.50	Steel	20.0	Scintillator	5.00
Yoke Barrel	1	90.00	Iron	50.0	RPC Gas	4.00
	1	240.00	Iron	200.0	RPC Gas	4.00
	15	140.00	Iron	100.0	RPC Gas	4.00
	1	240.00	Iron	200.0	RPC Gas	4.00
Yoke Plug	1	280.00	Iron	240.0	RPC Gas	4.00
Yoke Endcap	18	140.00	Iron	100.0	RPC Gas	4.00

4.1. Electromagnetic Calorimeter

The ECal is a highly segmented tungsten sampling calorimeter with silicon as the sensitive material. The innermost layer of the ECal consists only of a sensitive layer. It is followed by 20 layers with an absorber thickness of 2.5 mm and another 10 layers with an absorber thickness of 5 mm. The absorber material is tungsten. Each layer consists of the absorber material followed by an air gap of 0.25 mm, 0.32 mm of silicon (sensitive), 0.05 mm of copper, 0.3 mm of kapton and another air gap of 0.33 mm. The cell size in all layers is $3.5 \times 3.5\,\mathrm{mm}^2$. The total material corresponds to approximately $1.0\,\lambda_\mathrm{I}$ or $25.7\,X_0$.

The ECal barrel consists of twelve modules with non-pointing gaps, shown in Figure 7(a).

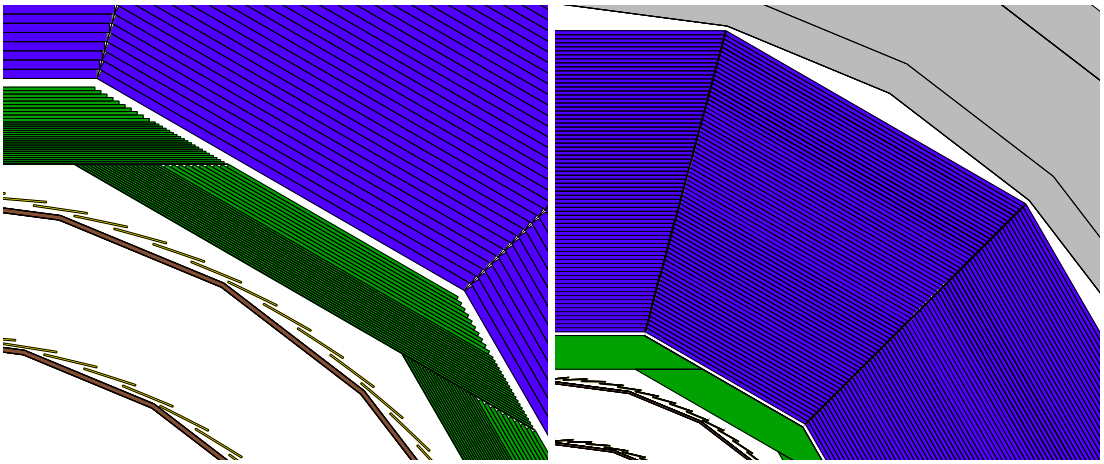

(a) (b)

Figure 7: Cut through the barrel region of the electromagnetic calorimeter (a) and the hadronic calorimeter (b), showing the layers and modules.

4.2. Hadronic Calorimeter

The HCal is a sampling calorimeter with polystyrene plates as the sensitive material. The polystyrene plates have a thickness of 5 mm and are segmented into $30 \times 30\,\mathrm{mm}^2$ cells. In addition to the sensitive layer and the absorber plates described below, there is an air gap of 1.5 mm in each layer. There is no material included to represent electronics, which does not affect the overall material budget significantly. The total gap size of 6.5 mm should be sufficient to accommodate sensitive material and electronics for all sampling calorimeter technologies currently being discussed [11].

There are 75 layers in the barrel with 10 mm tungsten absorber plates arranged in twelve modules with pointing gaps (see Figure 7(b)). The total material corresponds to $7.9\,\lambda_\mathrm{I}$.

In the endcaps there are 60 layers with 20 mm steel plates as absorber material, which corresponds to $7.6\,\lambda_\mathrm{I}$. This amount of material does provide sufficient absorption for hadronic showers at CLIC energies [12].

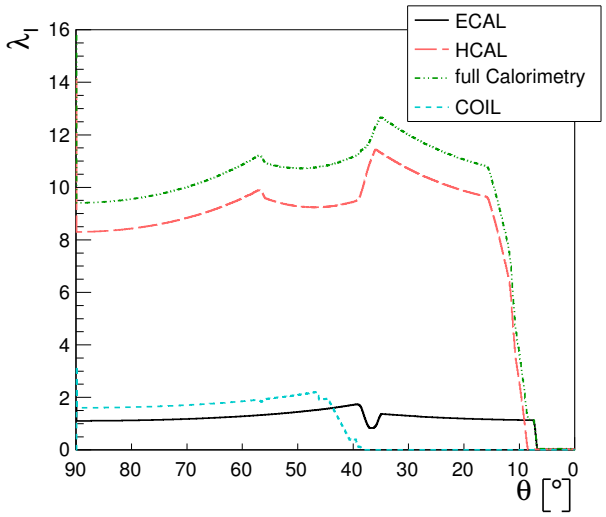

Figure 8: Nuclear interaction lengths λ_I in the calorimeters and coil with respect to the polar angle θ.

Table 10: Materials and corresponding thicknesses d in the RPC layers used in the instrumented yoke.

Material	d [mm]
Aluminium	1.0
Air	3.5
Pyrex Glass	2.0
RPC Gas	2.0
Pyrex Glass	2.0
Air	3.5
Aluminium	1.0

4.3. Instrumented Yoke

The detector is surrounded with an iron return yoke, which shields the experimental area from the magnetic field as well as radiation. It is instrumented with double-layers of resistive plate chambers (RPC) to help identify muons.

Each layer consists of two of the RPC layers described in Table 10, followed by an air gap of 10 mm and the absorber material. There are 18 layers in the barrel and the endcap with 100 mm of iron as absorber material in each layer. The first barrel layer has only 50 mm of iron to give a finer sampling directly after the coil. The second and the last absorber layer in the barrel are twice as thick, in order to take the stress.

Unlike the barrel, the yoke endcap begins with an absorber layer and ends with a sensitive layer. The 18 endcap layers have an absorber plate of 100 mm of iron and are instrumented like the barrel layers.

In addition a yoke plug fills the gap between HCal and yoke in the endcap region inside of the coil. It is instrumented with an RPC double-layer between two iron layers of 150 mm and 90 mm thickness.

An efficient muon identification can be achieved with fewer instrumented layers [13], thus, the overall size of the detector could be reduced. This is taken into account in the reconstruction by ignoring all the hits created in certain layers.

5. Solenoid and Magnetic Field

The superconducting coil is modelled as an aluminium cylinder, which represents the conductor and the mandrel. It is surrounded by a vacuum layer and a steel layer, which represent the

vacuum vessel. The vaccum vessel is closed by steel at its ends. The total thickness of the coil corresponds to approximately 1.5 λ_I. An overview of the parameters of the coil is shown in Table 11.

The solenoidal magnetic field is a homogeneous field of 5 T parallel to the detector axis throughout the volume inside of the coil. The field outside of the coil is 1.5 T pointing in the opposite direction of the inner field. There is no field beyond the end of the coil in z-direction.

Table 11: Description of the coil elements. For all elements the material, the longitudinal extent in one half of the detector $z_{\text{min/max}}$ and the radial extent $r_{\text{min/max}}$ are given.

Material	z_{min} [mm]	z_{max} [mm]	r_{min} [mm]	r_{max} [mm]
Steel	0	3515	2770	2800
Vacuum	0	3515	2800	2910
Aluminium	0	3395	2910	3344
Vacuum	0	3515	3344	3531
Steel	0	3515	3531	3571
Vacuum	3395	3515	2910	3344
Steel	3515	3575	2770	3571

6. Beam Pipe and Forward Region

6.1. Luminosity Calorimeter

The LumiCal extends the coverage for the identification of electromagnetic showers down to 64 mm, which corresponds to an opening angle of about 35 mrad. It is placed behind the ECal at a z-position of 1805 mm. The outer radius of 240 mm creates enough overlap with the ECal to avoid a gap in the coverage.

The instrumentation is very similar to the one of the ECal described in section 4.1. It also consists of two sections with different absorber thicknesses. The first 20 layers have a tungsten thickness of 2.71 mm and the last 15 layers have a tungsten thickness of 5.43 mm. Each layer consists of the absorber material followed by 0.32 mm of silicon (sensitive), 0.05 mm of copper, 0.3 mm of kapton and an air gap of 0.33 mm. The cell size is 3.5×3.5 mm^2 and the total material corresponds to 1.4 λ_I or 34.8 X_0.

A tube of G10 with a thickness of 50 mm is placed around the LumiCal as a placeholder for readout electronics.

6.2. Beam Calorimeter

The BeamCal completes the forward coverage of the electromagnetic calorimeters. It is has an outer radius of 130 mm and it starts at a z of 2486 mm. The BeamCal has two holes for the incoming and outgoing beam pipes. The radius of the hole for the incoming beam pipe is 2.55 mm and the radius for the outgoing beam pipe is 24.91 mm, which corresponds to an

opening angle of 10 mrad. This opening angle is enough to avoid the majority of the coherent pair background [14].

The BeamCal consists of 50 layers of 2.71 mm tungsten, 0.32 mm of silicon (sensitive), 0.05 mm of copper, 0.3 mm of kapton and an air gap of 0.33 mm. Like the other electromagnetic calorimeters, the sensitive layer is segmented into $3.5 \times 3.5\,\text{mm}^2$ cells.

A graphite layer of 100 mm is placed in front of the BeamCal in order to reduce the number of backscattered particles. The position in z of the BeamCal including the graphite mask is thus 2386 mm.

Table 12: Parameters for the forward calorimeter layers. The number N_{Layers} of identical layers , the total thickness d_{Layer} of each layer, the absorber material, its thickness d_{Abs}, the sensitive material and its thickness d_{Sens} are given.

	N_{Layers}	d_{Layer} [mm]	Absorber	d_{Abs} [mm]	Sensitive	d_{Sens} [mm]
LumiCal	20	3.71	Tungsten	2.71	Silicon	0.32
	15	6.43	Tungsten	5.43	Silicon	0.32
BeamCal	50	3.71	Tungsten	2.71	Silicon	0.32

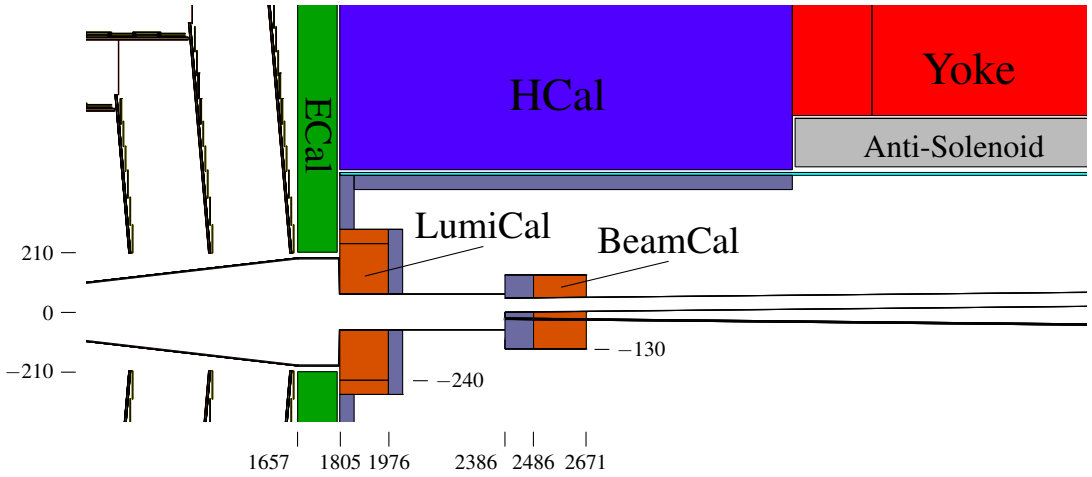

Figure 9: Layout of the forward region. The BeamCal and the LumiCal are shown together with the forward part of the beam pipe, the support tube and several shielding and mask elements. All values are given in millimeter.

6.3. Beam Pipe

The central part of the beam pipe is made of beryllium because of its low radiation length. It has an outer radius of 25 mm and a thickness of 0.5 mm. The conical parts and the elements in the far forward region are made of steel. The beam pipe becomes conical at a z of 260 mm with an opening angle of 6.6°. The thickness of the conical beam pipe is 4 mm in radial direction. It has

been found that this amount of steel effectively removes most of the backscattered particles that are created from the machine-induced-backgrounds in the far-forward region of the detector [15]. The beam pipe reaches a radius of 190 mm at the front face of the ECal and then becomes cylindrical again. This radius is small enough to allow an opening scenario of the detector where the vertex detector is removed together with the beam pipe.

The thickness of the beam pipe in front of LumiCal is 1 mm. A cylindrical beam pipe with an outer radius of 63 mm and a thickness of 1 mm is inside of the LumiCal and continues to the front face of the BeamCal. Two beam pipes which are centered around the incoming and outgoing beam axis are placed inside of the BeamCal holes and continue until the end of the detector.

A detailed study of the forward region, which was not forseen with this detector model, would require to change the beam pipe between LumiCal and BeamCal into a conical shape. It should then open up to the full acceptance of the BeamCal of 130 mm. It would be also required to close the beam pipe in front of the BeamCal, leaving only holes for the smaller incoming and outgoing beam pipes.

A detailed overview of all beam pipe elements is given in Table 13.

Table 13: Parameters for the beam pipe parts. Each part is a cylinder barrel or cone positioned between z_1 to z_2, the radii $r_{1/2}^{\text{in/out}}$ are the inner and outer radii at position $z_{1/2}$ respectively.

Material	z_1 [mm]	z_2 [mm]	r_1^{in} [mm]	r_2^{in} [mm]	r_1^{out} [mm]	r_2^{out} [mm]
Beryllium	0	230	24.5	24.5	25.0	25.0
Steel	230	260	24.5	24.5	25.0	28.5
Steel	260	1656	24.5	186.0	28.5	190.0
Steel	1656	1800	186.0	186.0	190.0	190.0
Steel	1800	1803	186.0	62.0	190.0	190.0
Steel	1803	1804	62.0	62.0	190.0	63.0
Steel	1804	2336	62.0	62.0	63.0	63.0
Steel[I]	2386	3575	2.0	2.0	2.5	2.5
Steel[O]	2386	3575	23.9	23.9	24.9	24.9

[I] Centered around the incoming-beam axis.
[O] Centered around the outgoing-beam axis.

6.4. Support Tube, Masks and Accelerator Components

All of the far-forward detectors and the final quadrupole (QD0) will be supported from a support tube which is mounted on the tunnel wall to fulfill the stability requirements on the QD0. This tube is simulated as a iron cylinder inside the HCal and yoke endcaps.

In addition there are several shielding elements to avoid backscatters from the BeamCal and other far-forward elements to reach the calorimeters. These are modelled as a layer of 50 mm of tungsten behind the LumiCal and the Ecal and right inside of the support tube within the HCal

endcap.

An anti-solenoid placed right outside of the support tube in the region of the yoke endcap. It is there to protect the QD0 magnet, which includes a permanent magnet, from the field of the central solenoid. The anti-solenoid is also modelled as an iron cylinder. The QD0, which would be placed around the incoming beam pipe behind the BeamCal is not represented in the detector simulation.

Table 14: Parameters of support tube and the anti-solenoid. The longitudinal extent in one half of the detector $z_{\text{min/max}}$ and the radial extent $r_{\text{min/max}}$ are given, as well as the material.

	z_{min} [mm]	z_{max} [mm]	r_{min} [mm]	r_{max} [mm]	Material
Anti-solenoid	3405	6195	510	680	Iron
Support tube	1805	6195	480	490	Iron

7. Simulation Software

The full detector simulation software SLIC v.2.9p8 is used for the CLIC CDR production. It uses GEANT4 v.9.3p2 to simulate the interaction of particles with the CLIC_SiD_CDR detector model. The physics list QGSP_BERT with a range cut of 0.1 mm is used as the physics model. A Lorentz boost of 10 mrad is applied to all particles during simulation, in order to simulate the effect of the beam crossing angle. This correction has to be applied because the physics events are generated as head-on collisions.

The detector model used in SLIC has been created from the compact detector description [16] with GeomConverter v.1.12 [17]. It is available online [18].

A. Materials

The following list of materials are used in the CLIC_SiD_CDR model and are either not available in or are differing from the default materials in GEANT4. The radiation length is given for those materials that are used in the tracking detectors.

A.1. Molecules

These materials are composed by number of atoms per element given in the parentheses.

Aluminium oxide aluminium (2) and oxygen (3) with a density of 3.89 g/cm^2.

Boron oxide boron (2) and oxygen (3) with a density of 2.46 g/cm^2.

Epoxy is a polymer made of hydrogen (44), carbon (15) and oxygen (7) with a density of 1.2 g/cm^2 and a radiation length of 316 mm.

Kapton is a polyimide made of carbon (22), hydrogen (10), nitrogen (2) and oxygen (5) with a density of 1.43 g/cm^2 and a radiation length of 284 mm.

PEEK (Polyether ether ketone) is a polymer made of carbon (19), hydrogen (12) and oxygen (3) with a density of 1.37 g/cm^2 and a radiation length of 303 mm.

Polystyrene is a polymer made of carbon (19) and hydrogen (21) with a density of 1.032 g/cm^2.

Quartz silicon (1) and oxygen (2) with a density of 2.2 g/cm^2.

ROHACELL31 (polymethacrylimid) is a foam consisting of carbon (9), hydrogen (13), oxygen (2) and nitrogen (1) with a density of 0.032 g/cm^2 and a radiation length of 12.92 m.

RPC gas is a mixture of tetrafluoroethane and isobutane consisting of carbon (209), hydrogen (239) and fluor (381) with a density of 0.0037 g/cm^2.

Silicon oxide silicon (1) and oxygen (2) with a density of 2.65 g/cm^2.

Sodium oxide natrium (2) and oxygen (1) with a density of 2.65 g/cm^2.

A.2. Mixtures

These materials are composed by mass fractions of several components.

Air 75.4% nitrogen, 23.4% oxygen and 1.2% argon with a density of 0.0012 g/cm^2.

Carbon carbon with a density of 2 g/cm^2 and a radiation length of 213 mm.

Carbon fiber 65.0% carbon and 35.0% epoxy with a density of 1.5 g/cm^2 and a radiation length of 281 mm.

Graphite carbon with a density of 1.7 g/cm^2.

G10 is a glass-reinforced plastic consisting of 8.0% chlorine, 77.3% quartz and 14.7% epoxy with a density of 1.7 g/cm^2 and a radiation length of 162 mm.

Pyrex glass is a borosilicate glass consisting of 80.6% silicon oxide, 13.0% boron oxide, 4% sodium oxide and 2.3% aluminium oxide with a density of 2.23 g/cm^2.

Steel 99.8% iron and 0.2% carbon with a density of 7.85 g/cm^2.

Tungsten used is an alloy of 93.0% tungsten, 6.1% nickel and 0.9% iron with a density of 17.8 g/cm^2.

Vacuum the beam pipe vacuum is hydrogen with a density of 10^{-8} g/cm^2.

References

[1] S. Agostinelli et al. Geant4 – A Simulation Toolkit. *Nucl. Instrum. Methods Phys. Res., Sect. A*, vol. 506(3) pp. 250–303, 2003.

[2] J. Allison et al. Geant4 developments and applications. *IEEE T. Nucl. Sci.*, vol. 53(1) pp. 270–278, 2006.

[3] Simulator for the Linear Collider (SLIC). Website: http://lcsim.org/software/slic/.

[4] K. Elsener, H. Gerwig, D. Schlatter, and N. Siegrist. CLIC Detector Concepts as described in the CDR: Differences between GEANT and Engineering Models. LCD Note in preparation, 2011.

[5] H. Aihara, P. Burrows, and M. Oreglia. SiD Letter of Intent. *ArXiv e-prints*, 2009.

[6] E. Brau, James et al. ILC Reference Design Report: ILC Global Design Effort and World Wide Study. 2007.

[7] M. Thomson. Particle Flow Calorimetry and the PandoraPFA Algorithm. *Nucl.Instrum.Meth.*, vol. A611 pp. 25–40, 2009.

[8] CLIC Conceptual Design Report, Volume 2, Chaper 13. 2011.

[9] C. Grefe. CLIC_SiD_CDR Tracking Performance. LCD Note in preparation, 2011.

[10] C. Grefe. Event Reconstruction in the CLIC_SiD_CDR Detector Model for the CLIC CDR Monte Carlo Mass Production. LCD Note in preparation, 2011.

[11] CLIC Conceptual Design Report, Volume 2, Chapter 8. 2011.

[12] P. Speckmayer and C. Grefe. Comparison of Performance of Hadronic Tungsten and Steel Sampling Calorimeters. 2010. LCD-Note-2010-001.

[13] E. van der Kraaij and B. Schmidt. Design of the Muon System for the CLIC Detectors. LCD Note in preparation, 2011.

[14] D. Schulte. High energy beam-beam effects in clic. oai:cds.cern.ch:385480. 1999.

[15] D. Dannheim and A. Sailer. Beam-induced Backgrounds in the CLIC Detectors. LCD Note in preparation, 2011.

[16] Compact Detector Description. Website: http://lcsim.org/software/geomconverter/apidocs/org/lcsim/geometry/compact/package-summary.html.

[17] GeomConverter. Website: http://lcsim.org/software/geomconverter/.

[18] The CLIC SiD CDR detector model. Website: http://lcsim.org/detectors/clic_sid_cdr.html.